

C.J. Guerrero Benavent¹, B. Franch^{1,2}, I. Moletto-Lobos¹, S. Saunier³, R. de los Reyes⁴, P. Schwind⁴, T. Storch⁴

¹Global Change Unit, Parc Científic, University of València (Paterna), 46980, Spain, cesar.guerrero@uv.es, belen.franch@uv.es, italo.moletto@uv.es,

²Dept. of Geographical Sciences, University of Maryland, College Park MD 20742, United States.

³Telespazio France, Satellite System and Operation, 26 Avenue JF Champollion, BP 52309, CEDEX 1, 31023 Toulouse, France

⁴German Aerospace Center (DLR), Remote Sensing Technology Institute, Photogrammetry and Image Analysis, Oberpfaffenhofen, 82234 Wessling, Germani



Introduction

- BRDF (Bidirectional Reflectance Function)** describes the anisotropy properties of a given surface by representing the surface reflectance for different viewing-illumination geometries. This function allows the directional reflectance normalization to a common geometry reducing noise in the time series.
- In the **multispectral domain**, BRDF methods rely on inverting the BRDF coefficients using several observations of a limited period of the same area from various sun-view geometries, what becomes challenging for medium-high resolution sensors with narrow angular sampling. **HABA (High resolution Adjusted BRDF Algorithm)** normalizes the Sen2like product operationally and is based on the coarse resolution MODIS BRDF parameters inferred from **VJB method**.
- There is **limited research concerning the applicability of kernel-based BRDF algorithms in the hyperspectral domain**. This work explores the adaptability of HABA algorithm to the hyperspectral domain based on the hypothesis of high correlated BRDF properties over nearby wavebands.
- First results of an intercomparison exercise based on an angular field campaign over an heterogeneous orange tree plantation in Valencia (Spain) are exposed here. HABA performance is compared to ASD FieldSpec Spectroradiometer field angular measurements using a goniometer and a crane to normalize satellite data from EnMAP.

Methodology

1 HABA (High resolution Adjusted BRDF Algorithm)

BRDF model: Ross-Li-Maignan model

F_1 = volume - scattering kernel

$$\rho(\theta_s, \theta_v, \phi) = k_0 + k_1 F_1(\theta_s, \theta_v, \phi) + k_2 F_2(\theta_s, \theta_v, \phi)$$

F_2 = geometric kernel

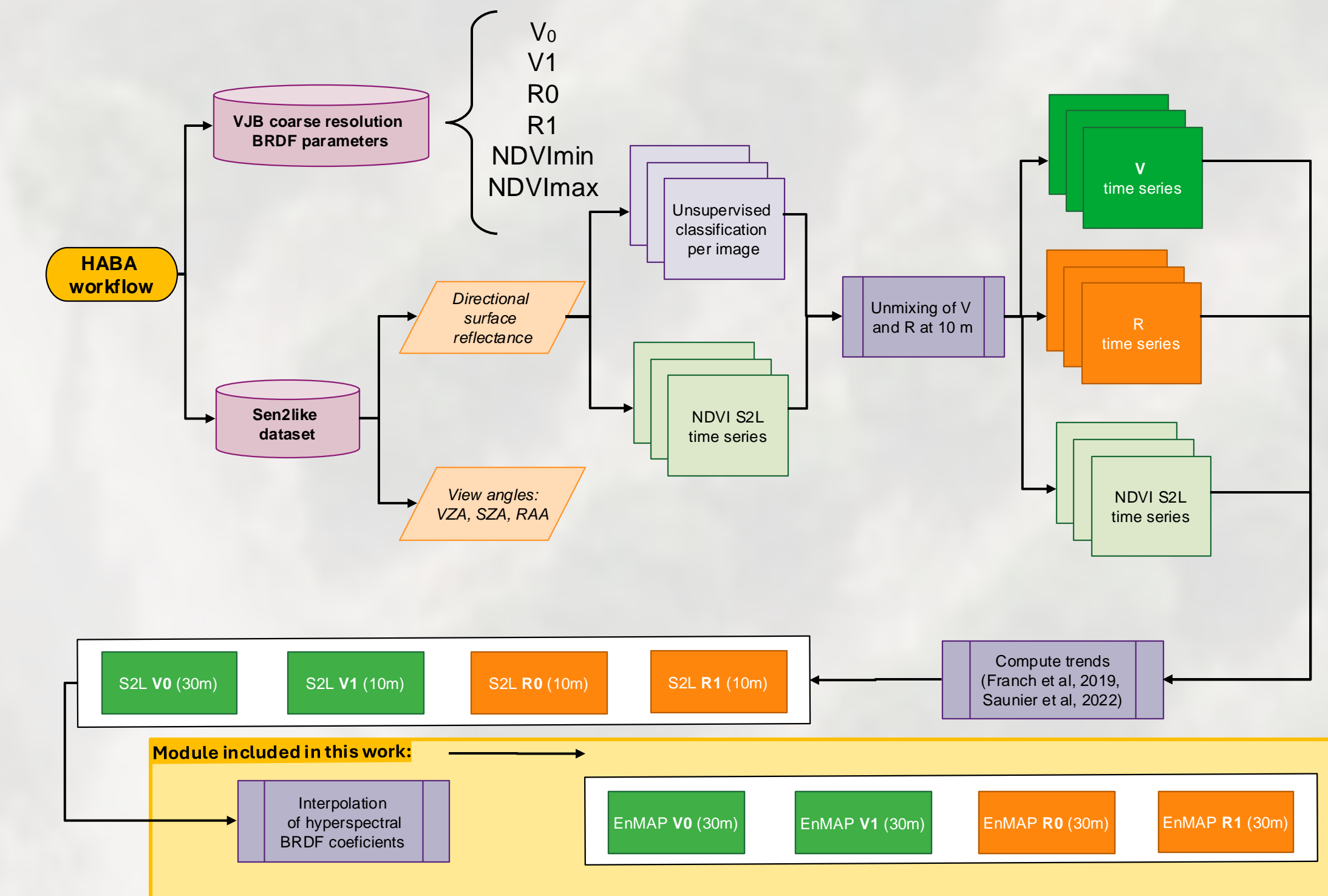
k_0, k_1, k_2 = free parameters

MODIS BRDF parameters, VJB method: Vermote et al. (2009)

$$V = k_0/k_1 = V_0 + V_1 NDVI$$

$$R = k_0/k_2 = R_0 + R_1 NDVI$$

Algorithm: Franch et al. (2009)



2 Field measurements: angular measurements performed on the Solar Principal Plane (SPP).

2.1 Goniometer measurements: (Tree scale)

8 hourly measurements to collect wide solar zenith angle variation at different view zenith angles: -50, -40, -30, -20, -10, 0, 10, 20, 30, 40, 50.

HOUR GMT +2	SOLAR ZENITH ANGLE
11:00	42.57°
12:00	31.36°
13:00	21.59°
14:00	16.45°
15:00	20.00°
16:00	29.2°
17:00	40.23°
18:00	51.79°



2.2 Crane measurements: (Field scale)

Crane measurements at different solar zenith angles and view zenith angles.

Nadir measurements (VZA = 0°):

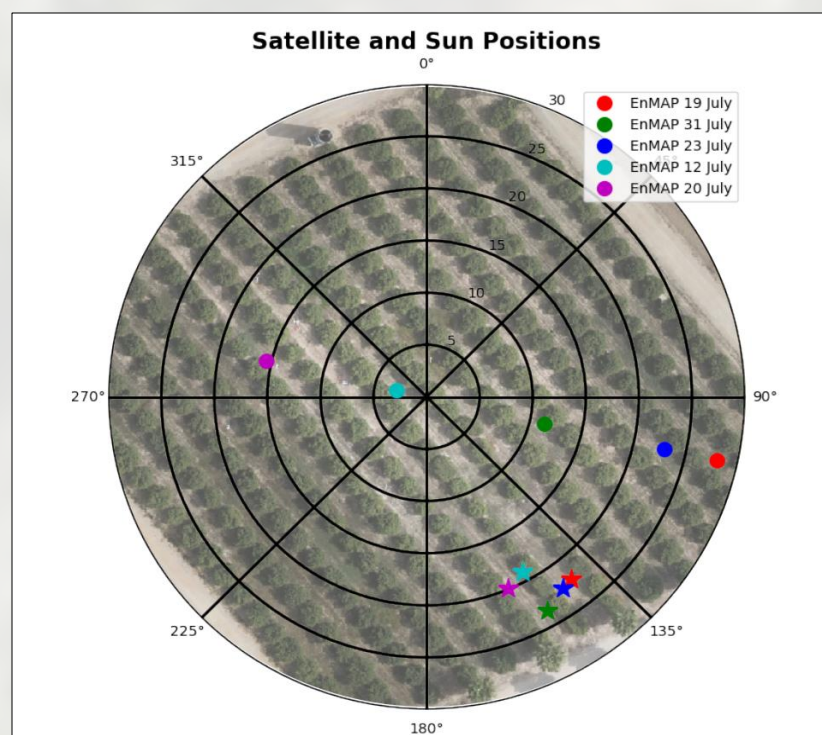
HOUR GMT +2	SOLAR ZENITH ANGLE
10:37	47.54°
11:30	37.44°
13:10	20.96°
14:30	17.76°
15:30	24.57°
16:30	34.84°
17:23	44.83°
18:18	55.47°

Angular measurements (VZA = 40°, 20°, 0°):

HOUR GMT +2	SOLAR ZENITH ANGLE
10:19 - 11:18	51.54° - 40.24°
13:40 - 16:00	18.76° - 29.88°
17:23 - 18:21	45.14° - 56.35°



2.3 Satellite acquisitions



DATE - HOUR GMT +2	VIEW ZENITH ANGLE	SOLAR ZENITH ANGLE
12/07/2024 - 13:29	2.9°	22.19°
19/07/2024 - 13:11	28°	23.41°
20/07/2024 - 13:36	15.6°	22.37°
23/07/2024 - 13:15	22.9°	19.07°
31/07/2024 - 13:21	11.4°	19.84°

2.4 Drone LIDAR measurements



3 Post-processing

- Compute goniometer and crane **hyperspectral BRDF coefficients** using multiple observations data.
- Simulate S2like **reflectance** with ASD goniometer measurements, **compute multispectral** goniometer BRDF coefficients and interpolate hyperspectral ones.
- Normalize EnMAP observations with all the different derived BRDF coefficients and compare.

Normalization equation

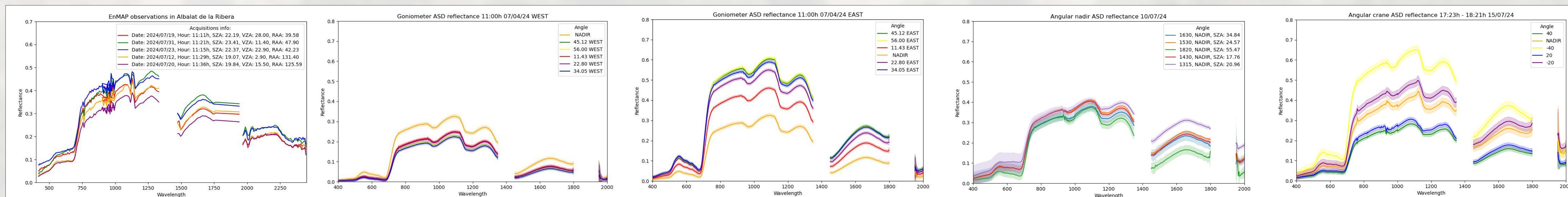
$$\rho_{norm}(\theta_{norm}, \phi_{norm}) = \rho(\theta_s, \theta_v, \phi) \frac{1 + VF_1(\theta_{norm}, \theta_{norm}, \phi_{norm}) + RF_2(\theta_{norm}, \theta_{norm}, \phi_{norm})}{1 + VF_1(\theta_s, \theta_s, \phi) + RF_2(\theta_s, \theta_s, \phi)}$$

Relative difference equation

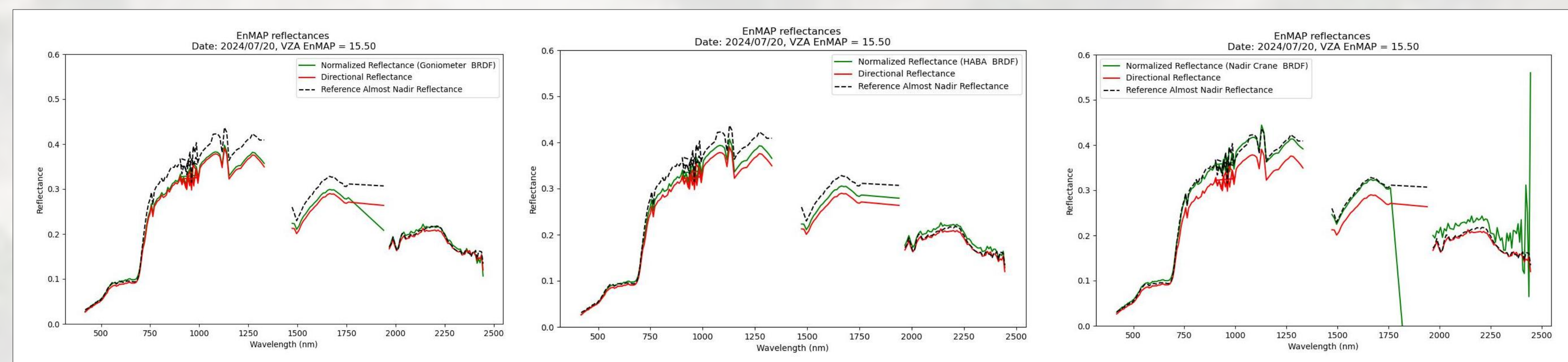
$$\Delta\rho = \frac{\rho_{preference} - \rho}{\rho_{preference}} \cdot 100$$

Results

Observation of BRDF effects:



Normalization of EnMAP reflectances: normalization of all EnMAP observations to the angular configuration of the 12th acquisition at VZA=2.9°



Date	Spectral Range	$\Delta\rho$ (%) (Dir.)	$\Delta\rho$ (%) (Norm. Gon.)	$\Delta\rho$ (%) (Norm. Gon. Int.)	$\Delta\rho$ (%) (Norm. Nadir Crane)	$\Delta\rho$ (%) (Norm. Crane)	$\Delta\rho$ (%) (Norm. HABA)
2024/07/19 SZA = 23.41° VZA = 28°	VISIBLE	-33.1	-15.82	-17.71	-27.61	-38.37	-29.69
	NIR	-5.2	-4.64	3.75	12.96	-8.11	-2.69
	SWIR1	1.6	12.55	10.94	10.24	-2.33	4.3
2024/07/31 SZA = 11.4° VZA = 11.4°	VISIBLE	0.5	13.11	11.29	-1.18	-4.03	3.27
	NIR	-12.5	-7.83	-7.92	-2.40	-14.42	-10.63
	SWIR1	-17.5	-11.43	-12.09	-11.27	-19.70	-15.22
2024/07/23 SZA = 19.07° VZA = 22.9°	VISIBLE	-15.8	-9.15	-9.66	-4.094	-18.10	-13.36
	NIR	-56.8	-38.22	-39.78	-48.20	-62.11	-51.87
	SWIR1	-16.4	-7.23	-7.64	-2.01	-20.02	-13.20
2024/07/20 SZA = 22.37° VZA = 15.5°	VISIBLE	-12.2	-1.34	-2.64	-1.94	-16.26	-8.51
	NIR	-15.1	-2.61	-3.82	-6.77	-19.53	-11.1
	SWIR1	5.7	-1.46	-2.31	-4.83	6.81	-0.32
	NIR	10.5	8.94	7.28	0.60	13.75	6.75
	SWIR1	11.9	8.79	7.86	1.35	13.58	7.22
	SWIR2	2.3	-0.5	-3.02	-18.00	3.50	-4.04

Conclusions

- The described field measurements have allowed to successfully retrieve the different scale anisotropy properties of the orange tree field.
- The **linear interpolation of the BRDF multispectral parameters** has demonstrated to be an **efficient and precise method to retrieve the hyperspectral BRDF parameters**, remarking the feasibility to adapt the HABA algorithm to the hyperspectral domain working towards an operational BRDF normalization algorithm for the upcoming CHIME mission.
- Angular crane measurements reduced the effectiveness of the BRDF correction, what could be caused by the position uncertainties when moving the crane or the non negligible deviation from the real SPP.

References

Vermote, E.; Justice, C.O.; Breon, F.M. Towards a Generalized Approach for Correction of the BRDF Effect in MODIS Directional Reflectances. IEEE Trans. Geosci. Remote Sens. 2009, 47, 898–908.
Franch, B., Vermote, E., Skakun, S., Roger, J. C., Masek, J., Ju, J., ... & Santamaria-Artigas, A. (2019). A method for Landsat and Sentinel 2 (HLS) BRDF normalization. Remote Sensing, 11(6), 632.

Acknowledgements This project was supported by:

COFRUT-MONITOR (ref AGROALNEXT/2022/046 funded by the Generalitat Valenciana)
Copernicus Hyperspectral Imaging Mission for the Environment (CHIME) L2 Algorithms and Processors Prototyping and Development (ref 4000142258/23/I-AG funded by ESA)